

## Spatial Distribution of Phase Singularities in Optical Random Vector Waves

L. De Angelis,<sup>1</sup> F. Alpeggiani,<sup>1</sup> A. Di Falco,<sup>2</sup> and L. Kuipers<sup>1,\*</sup>

<sup>1</sup>*Center for Nanophotonics, AMOLF, Science Park 104 1098 XG Amsterdam, The Netherlands*

<sup>2</sup>*SUPA, School of Physics and Astronomy, University of St Andrews, North Haugh, St Andrews KY16 9SS, United Kingdom*

(Received 20 May 2016; published 23 August 2016)

Phase singularities are dislocations widely studied in optical fields as well as in other areas of physics. With experiment and theory we show that the vectorial nature of light affects the spatial distribution of phase singularities in random light fields. While in scalar random waves phase singularities exhibit spatial distributions reminiscent of particles in isotropic liquids, in vector fields their distribution for the different vector components becomes anisotropic due to the direct relation between propagation and field direction. By incorporating this relation in the theory for scalar fields by Berry and Dennis [Proc. R. Soc. A **456**, 2059 (2000)], we quantitatively describe our experiments.

DOI: 10.1103/PhysRevLett.117.093901

Finding correlations in chaotic systems is the first step towards understanding them. Many are the fields where such predictions could be exploited, from weather forecasts to economic modeling [1,2]. The study of random phenomena is a topic of great interest and inspiration for many branches of physics as well. In electromagnetism, for example, random wave fields have been a topic of intense studies for decades, an outstanding example being the Anderson localization of light [3]. More recently the scientific interest in random wave fields has continued intensively, ranging from useful techniques such as non-invasive imaging with speckle correlation [4] to fascination concerning the observation of rogue waves in optical fields [5,6]. Zooming into the structure of a random wave field, attention has been pointed to the deep-subwavelength dislocations known as phase singularities [7].

Phase singularities are locations in which the phase of a scalar complex field is not defined. In two-dimensional fields these locations are points in the plane. Although they are just a discrete set of points, phase singularities can describe the basic properties of the field in which they arise. For this reason they are widely studied in wave fields [8–14], as well as in many areas of physics, where they are better known as topological defects in nematics [15] or as vortices in superfluids [16].

For a single frequency phase singularities are fixed in space, and their spatial distribution in a scalar field of monochromatic random waves has been analytically modeled by Berry and Dennis [17]. The hallmark of such a distribution is a clear pair correlation, reminiscent of that of particles in liquids. By realizing random wave ensembles in microwave billiards [18–20], the correlation of phase singularities was tested for a field perpendicular to the plane of the billiard, showing excellent agreement with the theoretical expectations [21]. For such a field and in that geometry indeed scalar theory was appropriate. However, electromagnetic waves are vectorial in nature, and in a

different framework it was already demonstrated how the presence of a spin degree of freedom can affect the correlation properties of a random field [22,23].

Here, we show how the vectorial nature of light affects the distribution of its phase singularities. By mapping the in-plane optical vector field measured above a chaotic resonator we investigate the distribution of phase singularities in two-dimensional random vector waves. We show that the distribution of phase singularities deviates from that for scalar random waves. This deviation is caused by the relation between the transverse field and the wave propagation direction. Thus, even when the considered vector field is equipartitioned with respect to both the in-plane polarization and the propagation direction, any specific choice of the field component directly leads to an anisotropic distribution of the contributing propagation directions. By treating this anisotropy with an analytical model we quantitatively explain our experimental observations. Finally, we show how an out-of-plane component that we construct from our in-plane fields obeys the predictions for scalar fields.

To generate optical random waves we inject monochromatic light ( $\lambda_0 = 1550$  nm) in a chaotic cavity: a silicon-on-insulator membrane enclosed by a planar photonic crystal with one input and one output waveguide [Fig. 1(a)]. Light is coupled through the input waveguide, exciting a transverse electric (TE) slab mode in the silicon membrane, which has its electric field vector in the membrane plane.

With our near-field microscope we map the in-plane components of the optical field in the cavity, which are in fact the only nonvanishing components of the electric field. The near field is locally converted and delivered to the far field through an optical fiber. A heterodyne detection scheme enables the measurement of the amplitude and phase [24]. With standard polarization optics we selectively detect the  $(E_x, E_y)$  Cartesian components of the in-plane electric field  $\mathbf{E}$  [25], thus gaining access to its vectorial

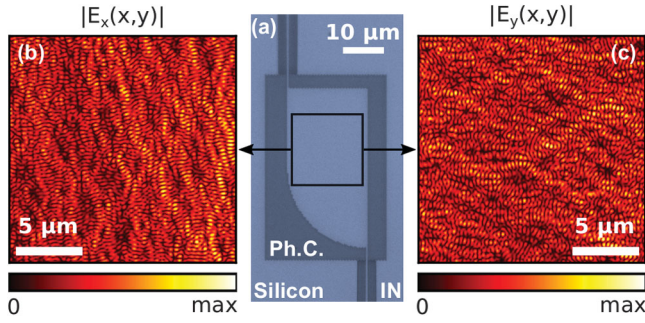


FIG. 1. Near-field measurement of the amplitude of the two Cartesian components  $E_x$  (b) and  $E_y$  (c) of the optical electric field in the chaotic cavity (optical micrograph shown) (a).

content. By scanning the surface of the sample we measure a two-dimensional map of the in-plane complex optical field above the cavity.

Figure 1 presents the measurements of the amplitude of  $E_x$  and  $E_y$ . The field pattern that results in the cavity can be thought of as a random superposition of plane waves [20]. We find that for the  $x$  and  $y$  components of the field the probability density function of the intensity is exponential [26], underlying the randomness. The near-field maps [Figs. 1(b) and 1(c)] depict the patterns resulting from the interference of light in the chaotic cavity. At first sight destructive and constructive interference occurs at random locations in the plane. On closer inspection a difference between the maps of the two field components catches the eye: the features of each pattern exhibit a preferred axis, related to the specific field component. A vertical stripy pattern with roughly  $1\text{--}2\ \mu\text{m}$  between the stripes is present in the  $E_x$  field. A modulation of the amplitude is observed along the stripes as well, characterized this time by a shorter length scale. The case of  $E_y$  is completely analogous, but rotated by  $90^\circ$ .

By separately measuring the Cartesian components of the electric field we implicitly established a criterion to depict a vector  $\mathbf{E}$  by using two scalar quantities ( $E_x$ ,  $E_y$ ), in which we can now seek for phase singularities [28]. Please note that such singularities cannot be found in the total intensity, which has no vanishing points. In a two-dimensional scalar complex field  $\psi(\mathbf{r})$ , phase singularities are points in which its phase  $\varphi$  is undefined. The phase circulates around the singular points, assuming all its possible values from  $-\pi$  to  $\pi$  [7]. Quantitatively, the line integral of  $\varphi$  along a path  $\mathcal{C}$  enclosing only one singularity yields an integer multiple of  $2\pi$ :

$$\int_{\mathcal{C}} d\varphi = 2\pi s, \quad (1)$$

where the integer  $s$  is called the topological charge of the singularity. The definition of the topological charge also gives us a powerful way to identify phase singularities. We calculate the integral of Eq. (1) along  $2 \times 2$  pixel loops at

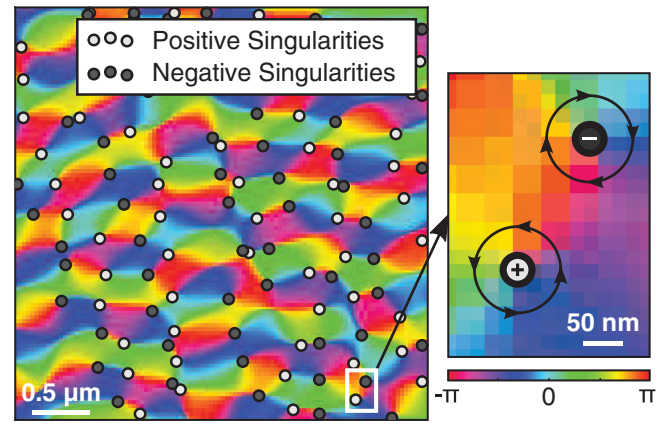


FIG. 2. False-color map of the measured phase of  $E_x$ . Phase singularities are represented (circles) with their topological charge:  $+1$  (positive) or  $-1$  (negative). The enlargement highlights how the direction of the circulation of the phase around the singular point determines its topological charge.

every point of the measured phase map, determining the position and topological charge of all the optical vortices in the field, with a spatial accuracy that is limited by the pixel size, which is approximately  $20\ \text{nm}$ . Figure 2 shows the phase singularities pinpointed in a subset of the phase map of  $E_x$ . Only topological charges of  $\pm 1$  are observed.

The distribution of optical vortices in the plane is rather disordered (Fig. 2), although already by eye a spatial correlation seems discernible if taking into account the topological charge. In order to unveil such a correlation we quantitatively characterize their spatial distribution. A natural way to do this is by calculating the pair correlation function

$$g(r) = \frac{1}{N\rho} \left\langle \sum_{i \neq j} \delta(r - |\mathbf{r}_j - \mathbf{r}_i|) \right\rangle, \quad (2)$$

where  $N$  is the total number of singularities,  $\rho$  is the average density of surrounding singularities, and  $\delta$  is the Dirac function. This function is directly related to the probability of finding two entities ( $\mathbf{r}_i$  and  $\mathbf{r}_j$ ) at a distance  $r$  from each other and is widely used in physics to describe discrete systems of various kinds [29].

Figure 3 presents  $g(r)$  calculated from our experimental data, specifically for the full data set of singularities of  $E_x$  [30]. The shape of the distribution function is highly similar to what is typically observed for a system of particles in a liquid [29]. After an initial dip  $g(r)$  oscillates about unity, with an amplitude that decreases as  $r$  is increased. The first peak, representative of a surplus of singularities, emerges at a distance of roughly half a wavelength. The decrease in amplitude of the oscillations describes the loss of correlation of the system. However, one peculiarity that we observe is definitely different compared to the case of a liquid:  $g(r)$  approaches a finite value for  $r \approx 0$ . This means that asymptotically there is a finite probability of finding

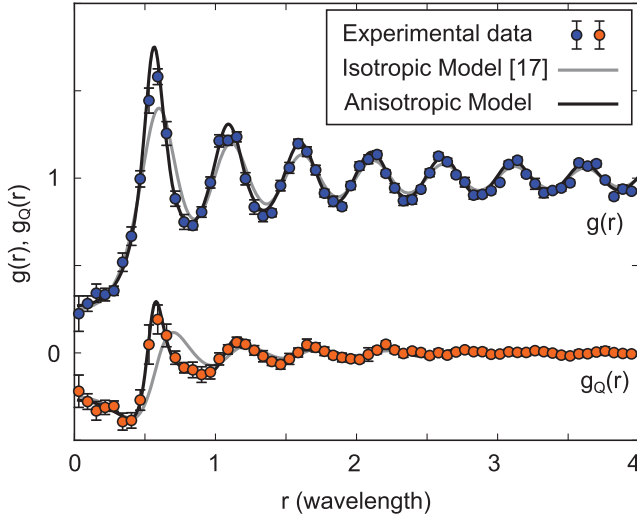


FIG. 3. Pair (blue) and charge (orange) correlation function of phase singularities in the measured field  $E_x$ . The gray line is the theoretical expectation for a scalar field of isotropic random waves [17]. Our data significantly deviate from such a theory, while a perfect agreement is obtained by considering a new model that includes directional anisotropies (black lines).

two vortices at the same location. While unusual this is in fact allowed by the zero dimensionality of optical vortices.

In analogy to what is typically done for ionic liquids [29], it is convenient to introduce a generalized expression of  $g(r)$  for a system of charged entities. In the charge correlation function  $g_Q(r)$  each vortex is weighted with its topological charge  $s$ :

$$g_Q(r) = \frac{1}{N\rho} \left\langle \sum_{i \neq j} \delta(r - |\mathbf{r}_j - \mathbf{r}_i|) s_i s_j \right\rangle. \quad (3)$$

The experimental result for  $g_Q(r)$  is also reported in Fig. 3, providing new information about our system. The main observation here is that  $g_Q(r)$  is approximately equal to  $-g(r)$  in the region  $r \approx 0$ , meaning that only singularities with opposite topological charge are likely to be indefinitely close to each other. This behavior is usually interpreted in terms of the reciprocal screening among critical points with opposite topological charge [31,32]. Notably, critical-point screening is related to the reduction of topological charge fluctuations inside a finite region with respect to the prediction for a collection of random charges [17,31,33].

In an influential paper [17] Berry and Dennis calculated the correlation functions of singularities in a scalar field  $\psi$ , modeled as a superposition of plane waves with the same momentum and random phases  $\delta_{\mathbf{k}}$ , i.e.,

$$\psi(\mathbf{r}) = \sum_{\mathbf{k}} a_{\mathbf{k}} \exp(i\mathbf{k} \cdot \mathbf{r} + i\delta_{\mathbf{k}}). \quad (4)$$

The model assumes that the wave amplitudes are isotropically distributed along a circle of radius  $k_0$  in Fourier space.

The results of this isotropic model are shown as solid gray lines in Fig. 3. Most of the key features of the experimental distribution are qualitatively accounted for by the model, but we clearly observe some deviation from the theory. The biggest difference is in  $g_Q(r)$ , where the first peak turns out to be narrower than in the theory, as well as significantly shifted towards lower distances. This is in contrast to what was observed for out-of-plane fields in microwaves billiards [21], where excellent agreement was found.

The origin of the observed discrepancies with respect to  $g(r)$  and  $g_Q(r)$  lies in the vector nature of the light. For the TE modes a direct relation exists between the selected in-plane field component and the direction of propagation: the modes will have no electric field component along the direction of propagation. Therefore, the choice of field component to be investigated (e.g.,  $E_x$  in Fig. 2) affects the distribution of the propagation directions that contribute to the wave pattern. Whereas the general model in Eq. (4) remains valid, the anisotropy of our system violates the assumption of isotropy [17], i.e., that  $a_{\mathbf{k}}$  only depends on the magnitude of  $\mathbf{k}$ . As a consequence, the field correlation function must display an additional dependence on the relative spatial orientation of the points.

We now calculate the correlation properties of the in-plane components of the field and of the corresponding singularity distribution, by including such an anisotropy in a modified version of the original model. Since for a TE mode  $\mathbf{E}(\mathbf{k}) \perp \mathbf{k}$ , the Fourier coefficients of the in-plane field components are effectively modulated by the sine of the angle  $\theta_{\mathbf{k}}$  enclosed by the direction of the considered field component and the in-plane wave vector  $\mathbf{k}$ . For this reason, we assume

$$E_j(\mathbf{r}) \propto \sum_{\mathbf{k}} \sin(\theta_{\mathbf{k}}) \exp(i\mathbf{k} \cdot \mathbf{r} + i\delta_{\mathbf{k}}), \quad j = x, y. \quad (5)$$

Note that the total intensity,  $E_x^2 + E_y^2$  remains isotropic.

The additional angular dependence in the Fourier expansion of Eq. (5) influences the correlation properties of the wave field. In particular, the spatial autocorrelation function of each field component,

$$C(\mathbf{r}) = \int d\mathbf{r}' E_j^*(\mathbf{r}') E_j(\mathbf{r}' + \mathbf{r}) = \frac{1}{2\pi} \int d\mathbf{k} |E_j(\mathbf{k})|^2 e^{-i\mathbf{k} \cdot \mathbf{r}}, \quad (6)$$

exhibits a dependence on the orientation  $\varphi$  of the vector  $\mathbf{r}$ :

$$C(\mathbf{r}) \doteq C(r, \varphi) = \frac{1}{2\pi} \int d\theta_{\mathbf{k}} \sin^2(\theta_{\mathbf{k}}) e^{-ik_0 r \cos(\theta_{\mathbf{k}} - \varphi)} \quad (7)$$

$$= \frac{1}{2} [J_0(k_0 r) + \cos(2\varphi) J_2(k_0 r)], \quad (8)$$

where  $J_n(x)$  is the Bessel function of order  $n$  and  $k_0$  is the wave number of the TE mode. This is in contrast to the case



of a fully isotropic scalar field, where  $C(\mathbf{r}) = J_0(k_0 r)$  [17]. The autocorrelation function of the field contains all the information needed to retrieve the pair and charge correlation functions of the phase singularities [26]. Analogously to  $C(r, \varphi)$ , the pair and charge correlation functions  $g^{(\text{an})}(r, \varphi)$  and  $g_Q^{(\text{an})}(r, \varphi)$  display a dependence on the spatial vector orientation  $\varphi$ . Since in the corresponding experimental quantities in Eqs. (2) and (3) the average is taken over all reciprocal orientations of the points, to compare the experimental data with the theoretical results, we average the latter over the polar angle:

$$g_Q^{(\text{an})}(r) = \frac{1}{2\pi} \int_0^{2\pi} d\varphi g_Q^{(\text{an})}(r, \varphi) \quad (9)$$

[and similarly for  $g^{(\text{an})}(\mathbf{r})$ ]. The black solid lines in Fig. 3 show the analytic outcome of such calculations (anisotropic model). A comparison between the experiment and the new model now exhibits an excellent qualitative and quantitative agreement. This confirms that the anisotropy in the direction distribution of random waves, intrinsic in the vector nature of optical wave fields, significantly affects the spatial distribution of phase singularities.

A further confirmation of the validity of our model comes from restricting the orientation of the spatial displacement vector  $\mathbf{r}$  to a limited range of values ( $\Delta\varphi = \pi/4$ ) around the directions perpendicular ( $\perp$ ) and parallel ( $\parallel$ ) to the field projection axis. In Fig. 4, we compare the results for both the experimentally calculated  $g_Q(\mathbf{r})$  and the restricted averages of Eq. (9) (anisotropic model). The two direction-dependent distribution functions

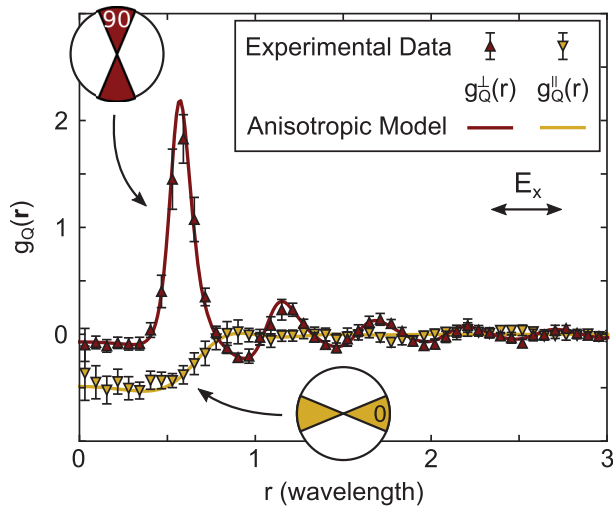


FIG. 4. Directional charge correlation function. We report the two illustrative cases of the direction perpendicular (red) or parallel (yellow) to the direction of the considered field component ( $E_x$ ). The distribution function strongly depends on the direction in the plane. The experimental data are represented by the triangles, while the lines show our modified model for anisotropic random waves, which perfectly fits the data.

show a completely different behavior, neither being equal to the isotropic  $g_Q(r)$  of Ref. [17], which, of course, does not display any orientation dependence. Several differences can be spotted between  $g_Q^{\parallel}$  and  $g_Q^{\perp}$ . First,  $g_Q^{\perp}(r)$  vanishes as  $r$  approaches zero, while  $g_Q^{\parallel}(r)$  does not. As a consequence, singularities of opposite sign are most likely to be arbitrarily close along the polarization direction. Second, in  $g_Q^{\perp}(r)$  there is an evident and positive peak, followed by a number of clear peaks with decreasing height. Sequences of same-sign singularities spaced by approximately half a wavelength are therefore expected along the direction perpendicular to the polarization (see also Fig. 2). Here, the loss of spatial correlation is slow compared to the direction parallel to the polarization, along which any correlation structure is immediately lost after the initial dip in  $g_Q^{\parallel}(r \approx 0)$ .

It is clear that the vector nature of the optical electric field impacts the spatial distribution of phase singularities. Interestingly, an out-of-plane field component would give us access to a quantity that behaves like a scalar. By Fourier transforming the measured complex fields  $E_x$  and  $E_y$  we can calculate the wave-vector space distribution of the magnetic field  $\mathbf{H} \propto \mathbf{k} \times \mathbf{E}$ . Fourier transforming back, we can thus construct a spatial map of  $H_z$  (up to a constant) [34], in which we identify the singularities and perform the same statistical analysis done for  $E_x$  and  $E_y$ .

The inset in Fig. 5 shows the amplitude of  $H_z(\mathbf{r})$  as constructed from our measured data. No anisotropy is evident in the resulting amplitude map, in contrast to what we observed for the constituent fields  $E_x$  and  $E_y$ . Figure 5 presents the distribution functions  $g(r)$  and  $g_Q(r)$  for the

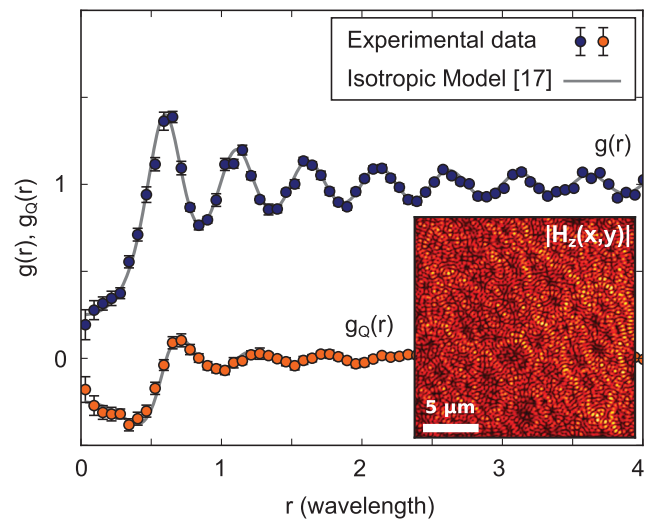


FIG. 5. Pair and charge correlation function of phase singularities in the constructed out-of-plane magnetic field  $H_z(x, y)$ . The distribution functions for singularities in this scalar field are in perfect agreement with the model for isotropic random waves [17]. In the inset is an amplitude map of  $H_z(x, y)$  (a.u.).

phase singularities in  $H_z$ , together with the theoretical model for isotropic random waves [17]. The agreement is in this case excellent. The direction-dependent distribution functions (not shown) do not exhibit any anisotropy.

When considering phase singularities in optical fields one needs to take into account that light is in general described as a vector wave. We studied the case in which the Cartesian components of an optical random field are separately considered as scalar quantities. We noticed how considering each field component goes hand in hand with directional anisotropies in the distribution of the propagation direction of random waves. This leads to significant consequences for the spatial distribution of optical vortices. As discussed by analyzing the experimental results supported by the analytical model, the differences become particularly dramatic when considering the angular dependence of the distribution. We stress that the anisotropic behavior that we analyzed in this Letter is a consequence of the vector nature of light and it is not related to the shape or dielectric constituents of the optical cavity that we used. For this reason, we believe that similar phenomena should arise every time a truly vectorial electromagnetic field is projected along one of its components.

The research data supporting this publication can be accessed at [35].

We thank Boris le Feber for useful discussions, and Pieter Rein ten Wolde and A. Femius Koenderink for critical readings of the manuscript. This work is part of the research program of the Netherlands Foundation for Fundamental Research on Matter (FOM) and the Netherlands Organization for Scientific Research (NWO). We acknowledge funding from ERC Advanced, Investigator Grant No. 240438-CONSTANS. A. D. F. acknowledges support from EPSRC (Grant No. EP/L017008/1).

\*kuipers@amolf.nl

- [1] D. S. Wilks and R. L. Wilby, *Prog. Phys. Geog.* **23**, 329 (1999).
- [2] L. Laloux, P. Cizeau, J.-P. Bouchaud, and M. Potters, *Phys. Rev. Lett.* **83**, 1467 (1999).
- [3] See A. Lagendijk, B. Van Tiggelen, and D. S. Wiersma, *Phys. Today* **62**, No. 8, 24 (2009) and references therein.
- [4] J. Bertolotti, E. G. van Putten, C. Blum, A. Lagendijk, W. L. Vos, and A. P. Mosk, *Nature (London)* **491**, 232 (2012).
- [5] C. Liu, R. E. C. van der Wel, N. Rotenberg, L. Kuipers, T. F. Krauss, A. Di Falco, and A. Fratalocchi, *Nat. Phys.* **11**, 358 (2015).
- [6] D. Pierangeli, F. Di Mei, C. Conti, A. J. Agranat, and E. DelRe, *Phys. Rev. Lett.* **115**, 093901 (2015).
- [7] J. F. Nye and M. V. Berry, *Proc. R. Soc. A* **336**, 165 (1974).
- [8] I. Freund, N. Shvartsman, and V. Freilikher, *Opt. Commun.* **101**, 247 (1993).

- [9] I. Freund, *Phys. Rev. E* **52**, 2348 (1995).
- [10] R. Bhandari, *Phys. Rev. Lett.* **89**, 268901 (2002).
- [11] D. M. Palacios, I. D. Maleev, A. S. Marathay, and G. A. Swartzlander, *Phys. Rev. Lett.* **92**, 143905 (2004).
- [12] S. Vignolini, M. Burreli, S. Gottardo, L. Kuipers, and D. S. Wiersma, *Opt. Lett.* **35**, 2001 (2010).
- [13] V. Peano, C. Brendel, M. Schmidt, and F. Marquardt, *Phys. Rev. X* **5**, 031011 (2015).
- [14] N. Rotenberg, B. le Feber, T. D. Visser, and L. Kuipers, *Optica* **2**, 540 (2015).
- [15] A. Fernández-Nieves, V. Vitelli, A. S. Utada, D. R. Link, M. Márquez, D. R. Nelson, and D. A. Weitz, *Phys. Rev. Lett.* **99**, 157801 (2007).
- [16] E. J. Yarmchuk, M. J. V. Gordon, and R. E. Packard, *Phys. Rev. Lett.* **43**, 214 (1979).
- [17] M. V. Berry and M. R. Dennis, *Proc. R. Soc. A* **456**, 2059 (2000).
- [18] M. Barth and H.-J. Stöckmann, *Phys. Rev. E* **65**, 066208 (2002).
- [19] Y.-H. Kim, U. Kuhl, H.-J. Stöckmann, and P. W. Brouwer, *Phys. Rev. Lett.* **94**, 036804 (2005).
- [20] H.-J. Stöckmann, *Quantum Chaos: An Introduction* (Cambridge University Press, Cambridge, England, 2006).
- [21] R. Höhmann, U. Kuhl, H.-J. Stöckmann, J. D. Urbina, and M. R. Dennis, *Phys. Rev. E* **79**, 016203 (2009).
- [22] J.-D. Urbina and K. Richter, *Adv. Phys.* **62**, 363 (2013).
- [23] A. T. Ngo, E. H. Kim, and S. E. Ulloa, *Phys. Rev. B* **84**, 155457 (2011).
- [24] M. L. M. Balistreri, J. P. Korterik, L. Kuipers, and N. F. van Hulst, *Phys. Rev. Lett.* **85**, 294 (2000).
- [25] M. Burreli, R. J. P. Engelen, A. Opheij, D. van Oosten, D. Mori, T. Baba, and L. Kuipers, *Phys. Rev. Lett.* **102**, 033902 (2009).
- [26] See Supplemental Material at <http://link.aps.org/supplemental/10.1103/PhysRevLett.117.093901>, which includes Refs. [17,27], for the Fourier decomposition of the measured fields, for the measured probability density function of the intensity of each field component, and for details on the derivation of the correlation functions in the anisotropic case.
- [27] J. W. Goodman, *Statistical Optics* (Wiley, New York, 1985).
- [28] M. V. Berry, *Proc. SPIE* **3487**, 1 (1998).
- [29] J.-P. Hansen and I. R. McDonald, *Theory of Simple Liquids* (Academic Press, London, 1990).
- [30] Similar results are observed for the case of the  $E_y$  field.
- [31] I. Freund and M. Wilkinson, *J. Opt. Soc. Am. A* **15**, 2892 (1998).
- [32] I. Freund, D. A. Kessler, V. Vasylov, and M. S. Soskin, *Opt. Lett.* **40**, 4747 (2015).
- [33] B. A. van Tiggelen, D. Anache, and A. Ghysels, *Europhys. Lett.* **74**, 999 (2006).
- [34] For a similar procedure in a different framework see, e.g., R. L. Olmon, M. Rang, P. M. Krenz, B. A. Lail, L. V. Saraf, G. D. Boreman, and M. B. Raschke, *Phys. Rev. Lett.* **105**, 167403 (2010).
- [35] <http://dx.doi.org/10.17630/c0539d3c-9c24-4446-bfff-9e6c04a1f7de>